The QCD phase diagram from Schwinger-Dyson Equations

Enif Gutiérrez[1], Aftab Ahmad[1,2], Alejandro Ayala[3], Adnan Bashir[1], and Alfredo Raya[1]
[1] *Instituto de Física y Matemáticas, Universidad Michoacana de San Nicolás de Hidalgo, Edificio C-3, Ciudad Universitaria, Morelia, Michoacán 58040, México.*
[2] *Department of Physics, Gomal University 29220, D. I. Khan, K.P.K., Pakistan.*
[3] *Instituto de Ciencias Nucleares, Universidad Nacional Autónoma de México, Apartado Postal 70-543, México Distrito Federal 04510, Mexico.*

We study the phase diagram of quantum chromodynamics (QCD). For this purpose we employ the Schwinger-Dyson equations (SDEs) technique and construct a truncation of the infinite tower of equations by demanding a matching with the lattice results for the quark-anti-quark condensate at finite temperature (T), for zero quark chemical potential (μ), that is, the region where lattice calculations are expected to provide reliable results. We compute the evolution of the phase diagram away from $T = 0$ for increasing values of the chemical potential by following the evolution of the heat capacity as a function of T and μ. The behavior of this thermodynamic variable clearly demonstrates the existence of a cross-over for μ less than a critical value. However, the heat capacity develops a singularity near $\mu \approx 0.22$ GeV marking the onslaught of a first order phase transition characterized by the existence of a critical point. The critical line continues until $\mu \approx 0.53$ GeV where $T_c = 0$ and thus chiral symmetry is finally restored.

PACS numbers: 25.75.Nq, 11.30.Rd, 11.15.Tk, 11.55.Hx

I. INTRODUCTION

The strong interaction sector of the standard model of particle physics involves a phase transition which is relevant to the evolution of the early universe. At low temperatures, the observable degrees of freedom of quantum chromodynamics (QCD) are color-singlet hadrons whereas at high energies or temperatures the interaction gets increasingly screened and hence weak, causing hadrons to break up into a new phase where the dominant degrees of freedom are the defining ingredients of perturbative QCD, namely, quarks and gluons. This is dubbed as *confinement-deconfinement phase transition*. The same physical picture prevails when chemical potential is increased. Experiments as well as lattice QCD computations for physical quark masses suggest that the temperature driven transition at zero chemical potential μ is not a thermodynamic singularity. Rather, it is a rapid but smooth crossover from the regime describable as a gas of hadrons, to the one characterized by quarks and gluons [1]. The μ driven transition at zero temperature T is qualitatively different. This regime cannot be accessed through lattice studies because the computations are hampered by the notorious sign problem. Nevertheless, a number of different model approaches indicate that the transition in this region is strongly first order [2].

Chiral symmetry restoration is another phase transition which is expected to occur when temperature and (or) chemical potential are sufficiently large. This happens when the dynamically generated component of quark masses vanishes. The pattern of chiral symmetry breaking at zero T and μ already provides evidence of the fact that large effective quark masses within light hadrons owe themselves primarily to the strength of the QCD interaction and dictate both their static and dynamic properties, see for example a recent review [3]. Its experimental implications for the elastic and transition form factors of mesons and baryons form an integral part of the planned program at the 12 GeV upgrade of the Thomas Jefferson National Accelerator Facility in Virginia [4]. As the strength of the QCD interaction diminishes with increasing T and μ, only the bare quark masses survive when these parameters exceed a critical set of values. This is referred to as the *chiral symmetry breaking-chiral symmetry restoration phase transition*.

In connection with these phase transitions, there are key questions which, to a considerable extent, provide the motivation for the heavy ion collision program at the Relativistic Heavy Ion Collider (RHIC) at Brookhaven National Laboratory (BNL), the Large Hadron Collider (LHC) at the European Centre for Nuclear Research (CERN) and the Compressed Baryonic Matter (CBM) experiment of the future Facility for Antiproton and Ion Research (FAIR) at Darmstadt. These can be summarized as follows :

1. Since the first order line originating at $T = 0$ in the QCD phase diagram cannot end at the $\mu = 0$ axis which corresponds to the starting point of the cross-over line, it must terminate somewhere in the midst of the phase diagram. This point is generally referred to as the critical end point. On one hand, it rests with the experiments to find observational evidence for it through extracting chemical and thermal freeze out temperatures, and on the other, the value of a sound theoretical prediction for its existence and location on the QCD phase diagram can hardly be exaggerated.

2. Are the two phase transitions, corresponding to deconfinement and chiral symmetry restoration, coincidental? As they both owe themselves to the

diminishing of the QCD interaction strength, one may expect them to chart out the same curve in the QCD phase diagram. However, its prediction and measurement continue to be essential as well as a challenging endeavor.

In this article, we concentrate on the exploration of the first point. Monte Carlo methods of lattice computations are severely handicapped off the $\mu = 0$ axis, because the fermion determinant becomes complex and thus standard Monte Carlo methods fail, as the integrand is no longer real and positive definite. However, these techniques can still be adapted to extract some information on the QCD phase diagram for $\mu \neq 0$ [5]. On the other hand, the fundamental field theoretical equations of QCD, namely, Schwinger-Dyson Equations (SDEs), have no such restriction. As their functional derivation makes no appeal to the smallness of the interaction strength, they provide an ideal, natural and unified framework to explore all the nooks and corners of the QCD phase diagram with ease. Moreover, the bare quark masses can be set as small as required and even studying the chirally symmetric Lagrangian is far from being herculean [6].

We study QCD phase diagram using the tools of SDEs at finite temperature and chemical potential. We work with two-flavor QCD with physical up and down current quark masses assuming isospin symmetry. The simplest two-point quark propagator is a basic object to analyze dynamical chiral symmetry breaking and confinement. At finite T and μ, we start from the general form of the quark propagator

$$\begin{aligned} S^{-1}(\vec{p},\tilde{w}_n) &= iA(\vec{p}^{\,2},\tilde{w}_n^2)\vec{\gamma}\cdot\vec{p} + i\gamma_4\tilde{w}_n^2 C(\vec{p}^{\,2},\tilde{w}_n^2) \\ &+ B(\vec{p}^{\,2},\tilde{w}_n^2)\,, \end{aligned} \tag{1}$$

where $\widetilde{w}_n = w_n + i\mu$ and $w_n = 2(n+1)\pi T$ are the Matsubara frequencies. $A(\vec{p}^{\,2},\tilde{w}_n^2)$, $B(\vec{p}^{\,2},\tilde{w}_n^2)$ and $C(\vec{p}^{\,2},\tilde{w}_n^2)$ are the scalar functions to be self consistently determined through solving the corresponding SDE

$$S^{-1}(\vec{p},\tilde{w}_n) = i\vec{\gamma}\cdot\vec{p} + i\gamma_4\tilde{w}_n + \Sigma(\vec{p},\tilde{w}_n)\,, \tag{2}$$

where $\Sigma(\vec{p},\tilde{w}_n)$ is the self-energy expressed in terms of the dressed gluon propagator $D_{\mu\nu}(\vec{p}-\vec{q},\Omega_{nl})$, with $\Omega_{nl} = w_n - w_l$, and the full quark-gluon vertex $\Gamma_\mu(\vec{q},\tilde{w}_l,\vec{p},\tilde{w}_n)$ as follows

$$\begin{aligned} \Sigma(\vec{p},\tilde{w}_n) &= T\sum_{l=-\infty}^{l=\infty}\int\frac{d^3q}{(2\pi)^3} g^2 D_{\mu\nu}(\vec{p}-\vec{q},\Omega_{nl}) \\ &\times \frac{\lambda^a}{2}\gamma_\mu S(\vec{q},\tilde{w}_l)\frac{\lambda^a}{2}\Gamma_\nu(\vec{q},\tilde{w}_l,\vec{p},\tilde{w}_n)\,. \end{aligned} \tag{3}$$

Here g^2 is the QCD interaction strength and the gluon propagator has the following general form in the Landau gauge

$$g^2 D_{\mu\nu}(\vec{k},\Omega_{nl}) = P^T_{\mu\nu} D_T(\vec{k}^{\,2},\Omega_{nl}) + P^L_{\mu\nu} D_L(\vec{k}^{\,2},\Omega_{nl})\,, \tag{4}$$

$P^{T,L}_{\mu\nu}$ being the transversal and longitudinal projectors defined as

$$\begin{aligned} P^L_{\mu\nu} &= \delta_{\mu\nu} - \frac{k_\mu k_\nu}{k^2} - P^T_{\mu\nu}\,, \\ P^T_{44} &= P^T_{4i} = 0, \quad P^T_{ij} = \delta_{ij} - \frac{k_i k_j}{\vec{k}^2}\,. \end{aligned} \tag{5}$$

Following the lead of Qin *et. al.* [7], we define

$$\begin{aligned} D_T(\vec{k}^{\,2},\Omega_{nl}^2) &= \mathcal{D}(T)\frac{4\pi^2}{\sigma^6}(\vec{k}^{\,2}+\Omega_{nl}^2)e^{-(\vec{k}^{\,2}+\Omega_{nl}^2)/\sigma^2}\,, \\ D_L(\vec{k}^{\,2},\Omega_{nl}^2) &= \mathcal{D}(T)\frac{4\pi^2}{\sigma^6}(\vec{k}^{\,2}+\Omega_{nl}^2)e^{-(\vec{k}^{\,2}+\Omega_{nl}^2+m_g^2)/\sigma^2} \end{aligned} \tag{6}$$

where $\sigma = 0.5$ GeV. There are a couple of noticeable differences in our adaptation of the above *ansatz* as will be clear along the way. Note that we take $D_L \neq D_T$ which is generally true when $T, \mu \neq 0$. The difference is governed by the gluon Debye mass m_g which enters only the longitudinal part of the gluon propagator. We take its value to be the lowest order hard thermal loop result $m_g^2 = 4g^2T^2/3$ [8] with $g = 1$. The effect of the Debye mass is negligible all the way through the thermal evolution, even when we use larger values of g. The role of the Debye mass is to help for the convergence of the solutions. We also allow $\mathcal{D}$ to be a function of temperature. With appropriate traces and simplifications, we obtain three coupled integral equations for $A(\vec{p}^{\,2},\widetilde{w}_n^2)$, $B(\vec{p}^{\,2},\widetilde{w}_n^2)$ and $C(\vec{p}^{\,2},\widetilde{w}_n^2)$ which are solved numerically. Convergence tests for the results allow us to sum over 14 Matsubara frequencies without sacrificing the accuracy of the results by more than 5%. Once we have calculated the quark propagator, we can evaluate the quark anti-quark condensate as :

$$\langle\bar{\psi}\psi\rangle = N_c\, T\sum_n\int\frac{d^3q}{(2\pi)^3}\mathrm{Tr}[S(\vec{q},\widetilde{w}_n)]\,. \tag{7}$$

However, notice that we have not yet said anything explicitly about $\mathcal{D}(T)$ (coming from the gluon propagator) or the quark-gluon vertex, or in fact their product which gets projected onto the quark self-energy. Where do we extract this information from? At this point, we introduce the most important input ingredient for our calculations. As we expect lattice computations to provide reliable results along the $\mu = 0$-axis of the QCD phase diagram, we make the following ansatz :

$$\mathcal{D}(T)\,\Gamma_\nu(\vec{q},\tilde{w}_l,\vec{p},\tilde{w}_n) = D(T)\,\gamma_\nu \tag{8}$$

and deduce $D(T)$ so as to reproduce the lattice results for the temperature dependent quark anti-quark condensate quoted in [9]. Note that for the chiral limit, we reproduce the results presented in [7] with appropriate modifications. In order to introduce a finite bare mass for the quarks, we use the fact that the mass function can be written as $M(\vec{p}^{\,2},\widetilde{w}_n^2) = B(\vec{p}^{\,2},\widetilde{w}_n^2)/A(\vec{p}^{\,2},\widetilde{w}_n^2)$ and then make the replacement $B(\vec{p}^{\,2},\widetilde{w}_n^2) \longrightarrow B(\vec{p}^{\,2},\widetilde{w}_n^2) +$

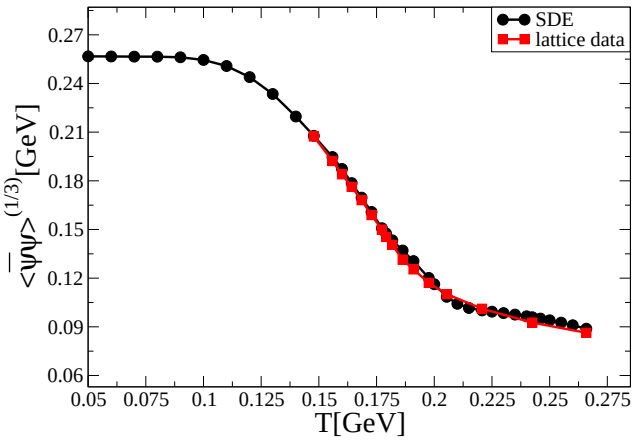

FIG. 1: Function $D(T) = a - bT^3 - c\tanh(d - eT^3)$ of Eq. (8) at $\mu = 0$ reproduces the lattice data [9] for the quark anti-quark condensate $\langle\bar{\psi}\psi\rangle$ very well, especially in the region of the phase transition.

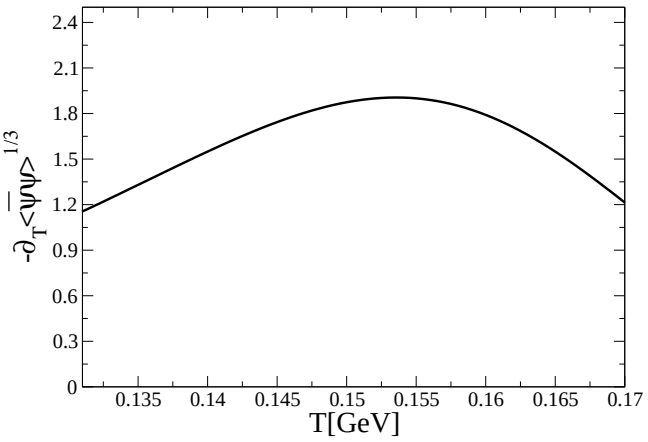

FIG. 2: Heat capacity $-\partial_T\langle\bar{\psi}\psi\rangle$ calculated from the SDE for $D(T)$ given by Eq. (9) as a function of temperature. Its maximum at $T_c \sim 0.153$ GeV agrees well with [9]).

$A(\vec{p}^2, \tilde{w}_n^2)m$. The self consistent solution of the coupled equations subsequently yields the quark propagator. With a fairly simple form of the function $D(T)$, i.e.,

$$D(T) = a - bT^3 - c\tanh(d - eT^3)\ , \qquad (9)$$

at $\mu = 0$ ($a = 2.17, b = 343.64, c = 1.76, d = 0.78$ and $e = 273.8$ with appropriate mass dimensions in GeV), lattice data is sufficiently well reproduced as shown in Fig. 1. One can draw the corresponding heat capacity curve given by $-\partial_T\langle\bar{\psi}\psi\rangle$ which yields a critical temperature of $T_c \approx 0.153\,\text{GeV}$, see Fig. 2. (compare it with $T_c = 0.154\,\text{GeV}$ reported in [9]).

We now extend our model and employ the same $D(T)$ as we evolve our results for $\mu \neq 0$. The gluon Debye mass becomes μ-dependent, i.e., $m_g^2 = (4T^2/3 + \mu^2/\pi^2)g^2$, also with $g = 1$. For increasing μ, we naturally observe chiral symmetry restoration at lower temperatures. This is depicted in Fig. 3 which confirms that the effect of incorporating the chemical potential μ tends to restore the chiral symmetry for lower temperatures. An important point to note is that as μ gets larger, a discontinuity starts to set in for the region where the critical temperature is located. It becomes increasingly pronounced with a relatively small variation of μ. Moreover, the slope of the curve increases drastically, so much that we eventually observe a vertical drop, as is evident in Fig. 3. This is a likely indicator of a physical effect. In order to quantify this change in the behavior of the heat capacity, we draw it as a function of temperature for different values of μ to locate the critical point. The result is shown in Fig. 4. The plots become narrower for increasing μ which helps locate the critical temperature with progressive precision. On the other hand, the height of the curve soon shoots up to infinity as evident from Fig. 4

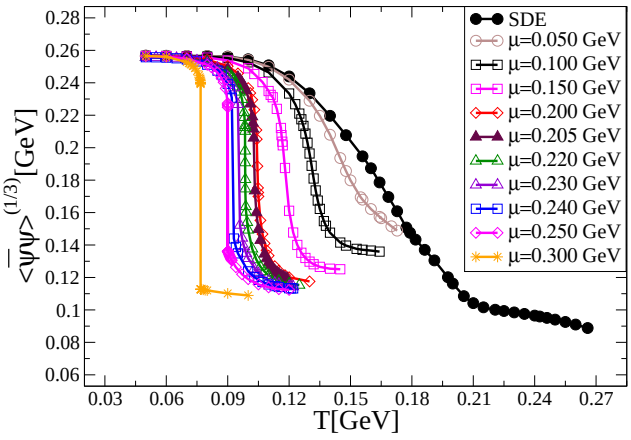

FIG. 3: The condensate for different values of μ as a function of temperature. For large μ, the curve develops a discontinuity which becomes more and more marked for increasing values of μ.

before the chemical potential reaches a value of about 0.22 GeV. We identify this thermodynamic singularity with the onslaught of a first order phase transition. Before that point is reached, the phase transition is a crossover. Notice from Fig. 3 that chiral symmetry remains broken beyond $\mu \approx 0.22GeV$, where the first order phase transition is triggered. Our numerical accuracy allows us to explore the chemical potential up to about 0.3 GeV. However, the trajectory of the points along the critical line is smooth enough to make a quadratic fit to estimate the value $\mu \approx 0.53\,\text{GeV}$ for zero temperature where chi-

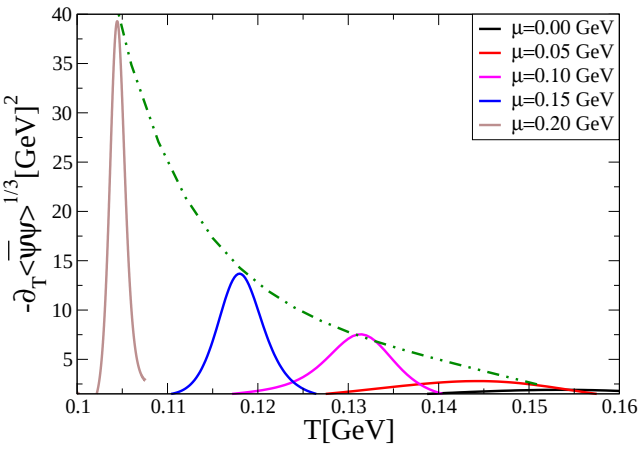

FIG. 4: We plot the heat capacity curve for the condensate as a function of temperature for different values of μ. The peak gives the critical point (μ_c, T_c). Note that the height of this thermodynamic variable shoots up to *infinity* for a sufficiently large μ, indicating a change in the order of phase transition.

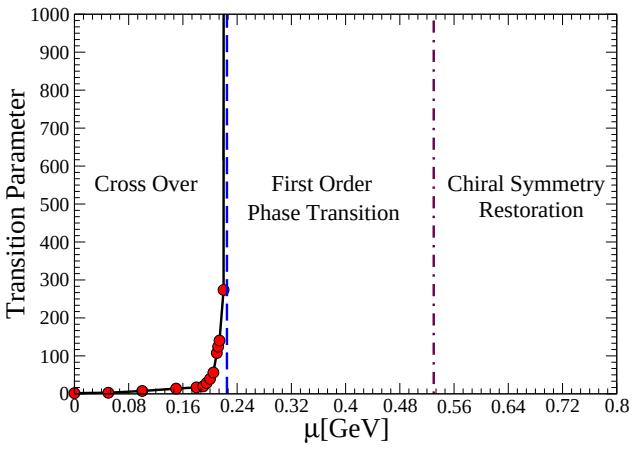

FIG. 6: This plot shows different regions of the QCD phase diagram as a function of the chemical potential μ. From $\mu = 0$ to the vertical dashed line at $\mu \approx 0.22$ GeV, the transition is a cross-over. The height of the heat capacity, the thermodynamic variable drawn on the vertical line, becomes singular as it approaches the dashed line, suggesting a change in the nature of phase transition from a simple cross-over to the first order phase transition. The chiral symmetry continues to be broken above $\mu \approx 0.22$ GeV, as evidenced from Fig. 3. However, it becomes numerically demanding to find the transition points. Chiral symmetry appears to be restored at $\mu \approx 0.53$ GeV, represented by a vertical dot-dashed line.

ral symmetry is finally restored, as shown in Fig. 5. All these characteristics are sketched in Fig. 6.

A few words of caution are here in order. The function $D(T)$ in Eq. (8) and the full quark-gluon vertex $\Gamma_\nu(\vec{q}, \tilde{w}_l, \vec{p}, \tilde{w}_n)$ surely depend on μ and a different choice of these quantities may change the position of the critical end point. Moreover, the fermion-boson vertex must be constructed from theoretical [10], as well as phenomenological [11] constraints. At finite T and (or) μ, the complexities involved are highly non-trivial but work has already begun in this direction [12]. We have performed preliminary studies to explore the nature of the confinement-deconfinement transition and have found that within this model the transition line follows the footsteps of the chiral symmetry breaking-restoration transition. This indicates that other transitions to quarkionic matter or a color locked phase, as the chemical potential increases, can only be described by incorporating additional ingredients to this model. While the above mentioned details will certainly be trimmed over the next few years, this letter shows that SDEs are an efficacious tool to explore the QCD phase diagram. We have used this tool to locate the critical end point as well as to provide clear signals of the cross over (near $\mu = 0$), and of a first order phase transition as we move away to sufficiently high values of μ, starting from lattice results for the finite temperature quark-antiquak condensate.

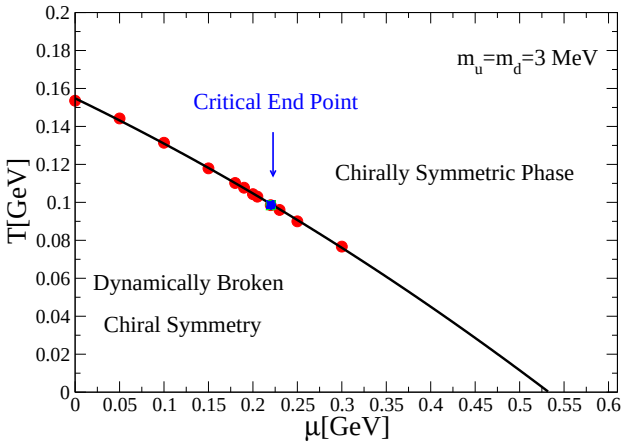

FIG. 5: We plot the phase diagram of QCD, indicating also the critical end point which corresponds to $\mu \approx 0.22 GeV$ and $T = 0.097 GeV$. Due to numerical difficulties above around $\mu \approx 0.3 GeV$, we adopted a quadratic numerical fit $f_1 + f_2 T + f_3 T^2$, to extrapolate our results to the $T = 0$ axis of the phase diagram which yields $\mu \approx 0.53$ GeV above which chiral symmetry is restored.

Acknowledgments: This work has been supported by CIC-UMICH grants 4.10 and 4.22, CONACyT grant numbers 82230 and 128534 and DGAPA-UNAM grant number IN103811.

[1] F. R. Brown, F. P. Butler, H.C. , N. H. Christ, Z. Dong, W. Schaffer, L. I. Unger and A. Vaccarino, Phys. Lett. C **65** 2491 (1990); A. A. Khan *et. al.*, Phys. Rev. D **63** 034502 (2001); Y. Aoki, G. Endrödi, Z. Fodor, S. D. Katz and K. K. Szabó, Nature **443** 675 (2006).

[2] M. Asakawa and K. Yazaki, Nucl. Phys. A **504** 668 (1989); A. Barducci, R. Casalbuoni, S. De Curtis, R. Gatto, and G. Pettini, Phys. Rev. D **41** 1610 (1990); A. Barducci, R. Casalbuoni, S. De Curtis, R. Gatto, and G. Pettini, Phys. Lett. B **231**, 463 (1989); A. Barducci, R. Casalbuoni, G. Pettini, and R. Gatto, Phys. Rev. D **49** 426 (1994); J. Berges and K. Rajagopal, Nucl. Phys. B **538** 215 (1999); A. M. Halasz, A. D. Jackson, R. E. Shrock, M. A. Stephanov, and J. J. M. Verbaarschot, Phys. Rev. D **58** 096007 (1998); O. Scavenius, A. Mocsy, I. N. Mishustin, and D. H. Rischke, Phys. Rev. C **64**, 045202 (2001); N. G. Antoniou and A. S. Kapoyannis, Phys. Lett. B **563** 165 (2003); Y. Hatta and T. Ikeda, Phys. Rev. D **67** 014028 (2003).

[3] A. Bashir, L. Chang, I. C. Cloët, B. El-Bennich, Y-X. Liu, C. D. Roberts, P. C. Tandy, Commun. Theor. Phys. **58** 79 (2012).

[4] *"Studies of Nucleon Resonance Structure in Exclusive Meson Electroproduction"*, I.G. Aznauryan *et. al.*, arXiv:1212.4891 [nucl-th] (2012).

[5] F. Karsch *et. al.*, Nucl. Phys. B, Proc. Suppl. 129-130, 614 (2004); E. Laermann, F. Meyer, M. P. Lombardo, *Making the most of Taylor expansion and imaginary chemical potential*, arXiv:1304.3247 [hep-lat] (2013).

[6] M. Harada, A. Shibata, Phys. Rev. D **59** 014010 (1999); T. Ikeda, Prog. Theor. Phys. **107** 403 (2002); C. S. Fischer, J. Luecker, J. A. Mueller, Phys.Lett. B **702** 438 (2011); A. Ayala, A. Bashir, C.A. Dominguez, E. Gutierrez, M. Loewe, A. Raya, Phys. Rev. D **84** 056004 (2011); S. Sasagawa, H. Tanaka, Phys. Rev. C **85** 045201 (2012).

[7] S.-x. Qin, L. Chang, H. Chen, Y-x. Liu, C. D. Roberts, Phys. Rev. Lett. **106** 172301 (2011).

[8] E. Braaten, A. Nieto, Phys. Rev. Lett. **73** 2402 (1994).

[9] A. Bazavov, T. Bhattacharya, M. Cheng, C. DeTar, H.T. Ding, S. Gottlieb, R. Gupta, P. Hegde, U.M. Heller, F. Karsch, Phys. Rev. **D85**, 054503 (2012).

[10] A. Kizilersu, M. R. Pennington, Phys. Rev. D **79** 125020 (2009); A. Bashir, A. Raya, S. Sanchez-Madrigal, Phys. Rev. D **84** 036013 (2011); A. Bashir, R. Bermudez, L. Chang, C.D. Roberts, Phys. Rev. C **85** 045205 (2012).

[11] L. Chang, C. D. Roberts Phys. Rev. C **85** 052201 (2012).

[12] A. Ayala, A. Bashir, Phys. Rev. D **64** 025015 (2001).